FUOYE Journal of Pure and Applied Sciences

Available online at www.fuoye.edu.ng

LITHOFACIES, PEBBLE MORPHOGENESIS AND PROVENANCE OF THE BIDA FORMATION, NORTHERN BIDA SUB-BASIN, NORTH-CENTRAL NIGERIA

[1]ADEPOJU, S.A, [2]Ojo, O.J. and [3]Akande, S.O

[1]Department of Geology and Mineral Sciences, Kwara State University, Malete, Kwara State.

[2]Department of Geology, Federal University Oye Ekiti, Ekiti State.

[3]Department of Geology and Mineral Sciences, University of Ilorin, Ilorin, Kwara State.

ARTICLE INFO

Received: 5 Aril, 2019

Accepted: 17 September, 2019

Keywords:
Lithofacies, Pebble Morphogenesis, Provenance, Fluvial, Bida Formation

Corresponding author:
olusola.ojo@fuoye.edu.ng

Abstract

The sedimentary provenance of Campanian Bida Formation sediments at Patigi and Baganko axis northern Basin Sub-Basin, North-central Nigeria were investigated using facies, pebble morphology, grain size and heavy mineral analyses. The goal is to contribute to a better understanding of regional tectonics and paleogeography of the Bida Basin. Lithofacies analysis revealed four basic sub-facies; clast-supported, massive conglomerate (Gcm), matrix-supported, massive conglomerate (Gmm), clast-supported, crudely bedded conglomerate (Gh), crudely stratified to massive sandstone (Se) that belongs to gravel bar (GB) fluvial architectural elements. The facies association is typical of Intraformational Conglomerate deposited in a shallow sandy and gravelly braided river system to a proximal alluvial plain. The similarity in average values of independent functions and dependent variables derived from pebble morphometric indices of Coefficient of Flatness (0.66; 0.65), Elongation Ratio (0.94; 0.95), Maximum Projection Sphericity (0.78; 0.76), Oblate-Prolate Index (-2.23; -2.17), Roundness (sub-angular to rounded) and Form (compact bladed, compact, very platy, very bladed, elongate and bladed) for sediments in Patigi and Baganko areas respectively suggest deposition of the sandstones in fluvial settings. The pebble imbrications paleo-flow indicator data ranges from 18 to 40°W in Patigi pointing to extensive low-sinuosity fluvial deposition towards western part of the Basin. The granulometric results of the interbedded sandstone samples vary from coarse to very coarse sand, poorly sorted to moderately sorted, coarse skewed to very fine skewed and mesokurtic to very platykurtic and thus classified texturally as gravelly sand to sandy gravel. The identifiable lithic clasts with tourmaline and zircon types in the sandstones within the study area point exclusively to derivation from a granitic and metamorphic origin. In conclusion, the lithofacies and architectural elements of the Bida Formation in the Patigi and Baganko are interpreted to represent channelized fluvial flow of gravel dominated braided rivers in proximal settings. The grain size and pebble morphology parameters with their scatter plots and paleoflow data show the sediments were deposited in a fluvial environment and sourced from eastern part of the Bida.

1.0 Introduction

The study area located in parts of Bida Basin north-central Nigeria is one of the hinterland sedimentary basins in Nigeria, having a sedimentary fill of about 4km [1], [2]. It is a northwest-southeast trending intracratonic structural depression adjacent and contiguous with Sokoto and Anambra Basins in the northwest and southeast respectively (figure 1). The Bida Basin is geographically subdivided into the northern and southern Bida sub-Basins to accommodate the fast and wide facies changes across its long and large areal extent [3]. Several authors have worked on the evolution of Bida Basin; [4] and [5] described it as a rift bounded tension structure produced by faulting associated

with the Benue Trough System and drifting apart of South America and Africa plates. This rift model was supported by [6] and [7]. [3], however suggested a wrench fault tectonic model for the origin of the basin. [8] regarded the basin as the north western extension of the Anambra basin both of which were major depo-centres during the third major transgressive cycle of southern Nigeria in the Late Cretaceous times. Interpretation of Landsat images, borehole logs, as well as geophysical data by [6] suggested that the basin is bounded by a system of linear faults trending NW – SE.

Stratigraphic framework in this basin has been along the geographic subdivision of the basin into north and south Bida basins. [9] and [10] established four stratigraphic horizons in the northern Bida Basin and these include; the basal Campanian-Maastrichtian Bida Formation (conglomerate, sandstone), Sakpe Ironstone, Enagi Formation (sandstone, siltstone, claystone) and Batati Ironstone (Figure 2). Their lateral equivalents in the southern Bida Basin are Lokoja Formation (conglomerate, sandstone), Patti Formation (sandstone, shale, claystone) and Agbaja Formation (ironstone).

Many researchers have contributed to the understanding of the depositional history and paleogeography of the southern part Bida Basin. [11] and [12] described and interpreted the origin of Agbaja Ironstone on the basis of its petrography and lithologic characteristics to be of the minnete type. [13] also investigated and reported the hydraulic characteristics of the sediments of both Lokoja and Patti formations and reported higher target of hydraulic exploration in the Lokoja Formation. [14] reported an occasional marine influence in the development of Campanian Lokoja Formation in the Southern Bida sub-Basin, thus interpreted the paleoenvironments of the sediments as alluvial fan to shallow marine.

Meanwhile, less research work has been documented in the northern Bida sub-Basin and the contributors includes; [3], [9], [15], [16], [17] and [18]. Therefore, this present study focuses on sedimentological attributes of the conglomerate and sandstone facies in the Patigi and Baganko (near river Niger) in northern Bida sub-Basin with the main aim to determine the provenance, palaeogeography and eventually reconstruct the palaeoenvironment of the sediments within the area.

2.0 Location, Materials and Methods

The investigated outcrops are recently exposed quarry sites located at Patigi (proposed Harman Patigi University) and Bakango (near Lafiagi) localities within longitudes and latitudes 08°42'53.5"N; 005°46'55.7"E and 08°54'29.4"N; 005°19'24.6"E respectively (Figure 1). The two (2) lithological sections exposed at each location were carefully studied bed by bed, logged and representative samples were obtained for laboratory analyses.

Clasts were carefully and randomly collected from the conglomerate and conglomeratic sandstones beds at each section to study and determine their morphological characteristics while the interbedded sandstones were subjected to the grain size distribution analysis. Paleocurrent measurement of the clasts in their original position were also taken and recorded. These sedimentological methods of investigation basically depend on determination of various independent and dependent functions of the pebbles and sediment grains have been used as indices for the determination of environment of deposition.

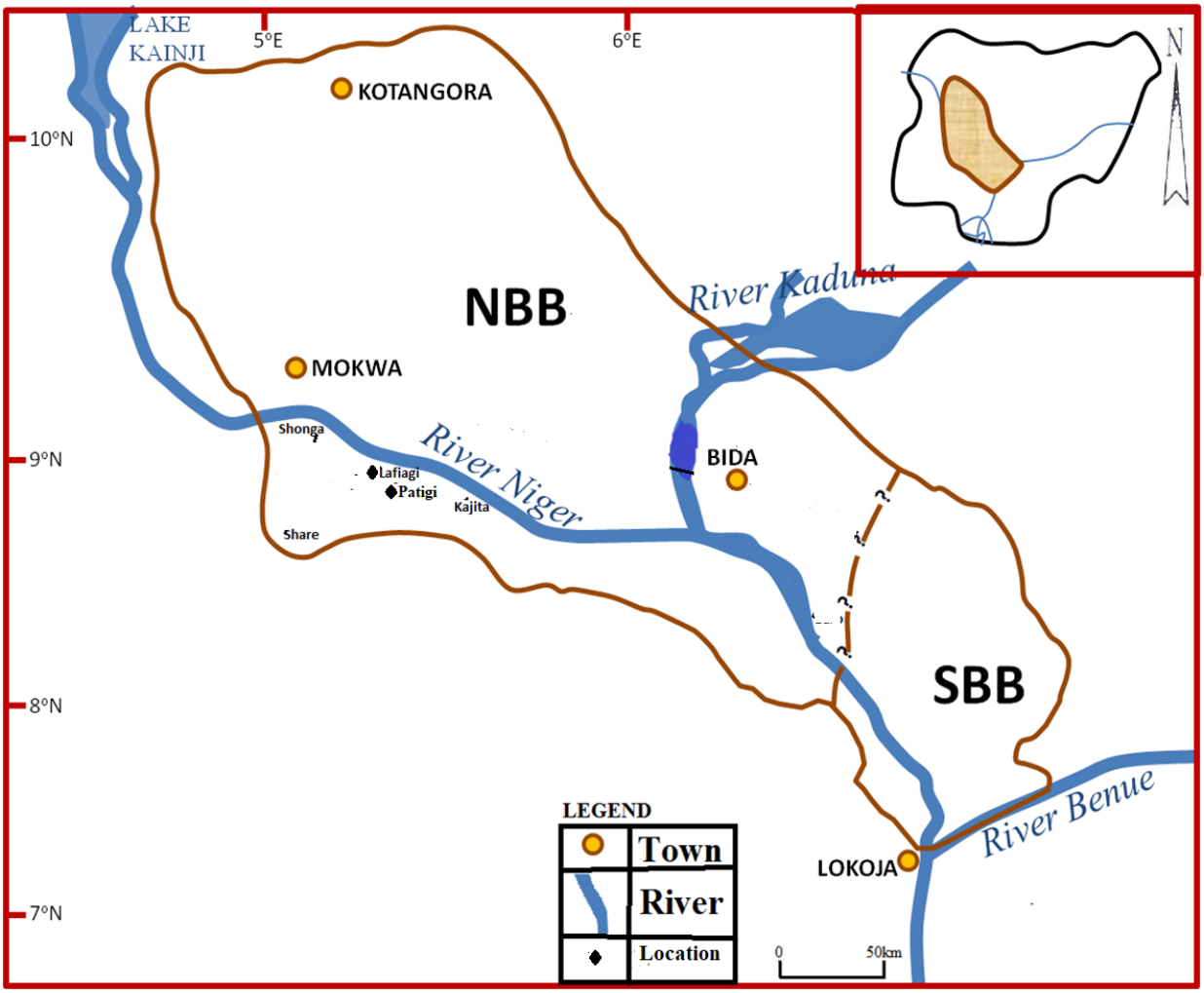

Figure 1: Map of the study area showing study location and important towns and the inset map of Nigeria showing the position of Bida Basin (Inset).

3.0 Facies Analysis

3.1 Lithofacies, Sub-facies and Interpretation

At each exposure, individual lithounits were identified based sediment texture and on gross lithology in detail. Each bed was given a facies name and a symbol following the classification scheme of [19, 20], [21], [22], [23] on the basis of observational physical characteristics. Generally, the exposed sediment of Bida Formation at the two (2) outcrop sections; Patigi (near River Niger) and Bakango (near Lafiagi) composed of distinct conglomerate and sandstone lithofacies which are further sub-divided into four (4) sub-facies; clast-supported, massive conglomerate (Gcm), matrix-supported, massive conglomerate (Gmm), clast-supported, crudely bedded conglomerate (Gh), crudely stratified to massive sandstone (Se) that are arranged into a distinctive coarsening upward sedimentation cycles (Figure 2).

3.1.1 Clast-supported, massive conglomerate (Gcm) sub-facies

The clast-supported, massive conglomerate (Gcm) sub-facies otherwise known as

Ortho-conglomerate [24], is moderately well sorted, composed of sub-rounded to rounded pebble size clasts and granules (0.3 to 14.0cm in diameter), mainly quartz and schist, commonly occurs within beds of 0.5 to 3.0 meters thick. Majority of the clasts with ordered imbricated fabric lie tangential to bedding (Figure 3a).

Gcm dominated the component, comprising 55% of total sub-facies present. Gcm sub-facies were observed in upper parts of the lithological sections exposed in southern parts of the proposed Harman-Patigi University, Patigi and northern part of Baganko village. The thickness of Gcm sub-facies bed implies the operation of mass-flows of considerable magnitude with rolling bedload of the large clasts along a bed and it's suggested to be a deposit from traction by a unidirectional current. The shape and size of the sandwiched clasts also reflects a high discharge and higher energy of the depositional current.

3.1.2 Matrix-supported, massive conglomerate (Gmm) sub-facies

This Matrix-supported, massive conglomerate (Gmm) sub-facies is generally supported by poorly sorted, coarse-grained sandstone filling the space between clasts (Figure 3b). It is otherwise referred to as Paraconglomerate by [24]. Individual beds of Gmm ranges between 0.2 and 1.0m thick with sharp bases and the clasts present are usually of size range between 1.7 and 8.7cm in diameter. The clasts sitting in a poorly sorted matrix are mostly sub-angular to rounded, non-imbricated granules to pebbles (mainly quartz and schist) which usually decrease upward in each cycle (Figure 3c).

Gmm comprises about 30% of the total sub-facies present within the area. Generation of Gmm sub-facies may be connected with the result of catastrophic flooding events, during which channels formed and they were filled with poorly sorted or unsorted coarse materials. Also, the occasional gradation of the sub-facies beds may indicates deposition from a single current as the energy and flow strength diminished [25].

3.1.3 Clast-supported, crudely bedded conglomerate (Gh) sub-facies

The clast-supported, crudely bedded conglomerate (Gh) is composed of few sub-angular to sub-rounded, poorly sorted gravel lenses that floats within the sand matrix with grading exhibiting an abrupt upward transition into Gcm and Gmm sub-facies (Figure 3b). The beds thickness ranges from 0.3 to 0.8m. In few occasions, Gh sub-facies consists of stratified gravels that commonly infill channelized erosive basal surfaces and the gradational top contact. It has the lowest component proportions among the sub-facies present with 5%. Gh sub-facies were observed as interbeddings within the Gcm and Gmm sub-facies and commonly passes upward into conglomerate sub-facies. Occasionally, the pebbly clasts form irregular bands on the erosional surface defining a bounding surface between the lower and upper bed as observed.

Due to the crudely bedded nature of Gh sub-facies, it is interpreted to represent the accretion of gravel in longitudinal bars which usually begins with the largest clasts as diffuse gravel sheets [21]. This attributes like Gcm and Gmm is a gravel- dominated braided rivers in a fluvial system according to [26] and [20].

3.1.4 Crudely stratified to massive sandstone (Se) sub-facies

The crudely stratified to massive sandstone (Se) sub-facies is composed of sands and minor silts, medium sorted and occur only at the lowermost beds of the studied sections (Figure 2). The bed appears ranges between 0.2m to 1.0m thick and commonly passes upward into conglomerate bed (Figure 3d).

It made up 10% lowest component proportions among the sub-facies present with. The presence of massive sandstone suggests an upper flow regime during transportation [19]. Presence of Sm sub-facies together with the conglomerate facies is suggestive of development of low sinuosity channel bars arising from channel switching and lack of point bar sedimentation [27, 28, 29].

3.2 Outcrop Facies Association, Architectural Elements, SandBody Geometry and Fluvial Styles

The outcrop facies association (OFA) is attempted to understand depositional environments and processes so as to determine the interrelationship of the facies present [19]. The lithofacies and sub-facies observed occurred typically as vertically stacked layers of coarsening–upward motif, laterally confined and lenticular bodies that characterize intraformational conglomerate outcrop facies associations. This intraformational conglomerate outcrop facies association represents channel lags that formed by migration of longitudinal and transverse bars during maximum discharge within a fluvial system [20]. And it can be interpreted to represent channelized fluvial flow of gravel dominated braided rivers (in proximal settings) according to [19].

The analysis of the outcrops using architectural element after [30] also supported the fluvial depositional styles suggested. The architectural element, gravel bars and bedforms (GB) elements characterized by lobate type geometry is interpreted as high energy braided system with low sinuosity and is typical of the Bida Formation.

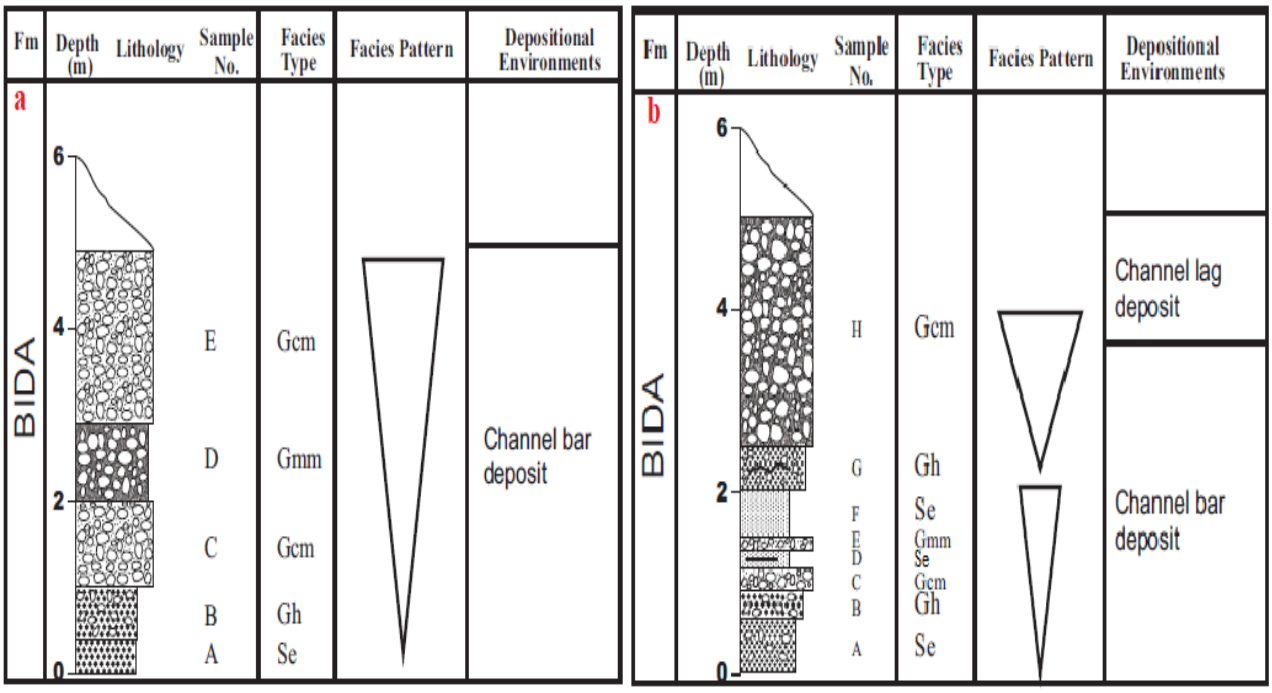

Figure 2: Lithological logs of outcrop sections at; (a) Patigi and (b) Baganko

Figure 3: Field photograph showing characteristic example of the sub-facies present within the study area; a and b are the photograph of typical sub-facies at Patigi while c and d are the photograph of typical sub-facies at Baganko.

4.0 Results

Results of all analytical techniques employed in the study are presented and discussed here. A critical assessment of each set of the results and their integration has aided the proper interpretation and useful discussions.

4.1 Pebble Morphometric Analysis

Over 200 various sizes of clast samples were randomly collected from both locations and screened to exclude the cracked or freshly broken prior to the morphometric analysis. The sizes of randomly selected clasts from the conglomerates fall within pebble and cobble classes according to [31] scale. The highly resistant pebbles were then selected, numbered, and subjected to the analysis to generate the statistical data. One hundred and twenty-nine (129) pebbles and cobbles of quartz and quartzite were finally measured and recorded. The pebble morphometry [32] involves measuring the pebbles' diameter using venier caliper to measure the long (L), intermediate (I), and short (S) axes of pebbles to determine the independent and dependent morphometric parameters. Clast roundness estimation based on the percentage of convex parts of a pebble along its external circumference was estimated with the aid of the [33] charts.

The independent variables include; the coefficient of flatness ratio (FR) and elongation ratio (ER) after [34], maximum projection sphericity index (M.P.S.I) and oblate-prolate index (OPI) after [35] while scatter plots of maximum projection sphericity index (M.P.S.I) versus oblate-prolate index (OPI), roundness (%) versus elongation ratio (ER) are the dependent variables. These statistical parameters have been employed by several past workers to evaluate and identify the depositional environment.

The results obtained from the pebble morphogenesis and the ranges are presented in tables 1 and 2. For the clast samples from Patigi (PAT 1D and 1E), the flatness ratio (FR) ranges from 0.46 to 0.88, elongation ratio (ER) range from 0.52 to 1.21, maximum projection sphericity index (M.P.S.I) ranges from 0.60 to 1.01, oblate-prolate index values range from 0.00 to -9.40 and roundness from 40 to 90% (sub-angular to well rounded). Meanwhile, clast samples from Baganko (BAK 1B, 1E, 1C and 1G) produces the following data; flatness ratio (FR) range from 0.33 – 0.88, mean elongation ratio (ER) range from 0.77 to 1.40, mean maximum projection sphericity index (M.P.S.I) ranges from 0.49 to 0.96, oblate-prolate index range from -20 to 6.67, roundness from 20 to 80% (angular to rounded) and clast form dominantly of compact bladed and compact with few very platy, very bladed and very few elongate and bladed (Figure 4).

Figure 4: selected pebbles for morphometric analysis

Table 1a: Pebble morphometric data of matrix-supported, massive conglomerate (Gmm) sub-facies in Patigi (PAT 1D)

S/N	L	I	S	F.R (S/L)	E.R (I/L)	M.P.S.I	O-P	Roundness	Form	R.F
1	1.70	1.60	1.30	0.76	0.94	0.85	-1.91	90	C	Quartz
2	2.30	2.00	1.50	0.65	0.87	0.79	-0.82	90	C	Quartz
3	2.40	2.00	1.70	0.71	0.83	0.84	0.51	90	CB	Quartz
4	2.00	2.20	1.60	0.80	1.10	0.83	-8.00	60	CB	Quartz
5	6.00	6.00	4.20	0.70	1.00	0.79	-3.50	60	C	Quartz
6	6.50	7.00	4.00	0.62	1.08	0.71	-4.31	70	C	Quartz
7	5.80	7.00	3.70	0.64	1.21	0.70	-6.83	40	VB	Quartz
8	3.20	2.70	2.30	0.72	0.84	0.85	0.40	70	C	Quartz
9	4.50	3.70	3.00	0.67	0.82	0.81	0.22	70	CB	Quartz
10	5.20	2.70	3.80	0.73	0.52	1.01	9.40	50	CB	Quartz
11	5.00	4.60	3.80	0.76	0.92	0.86	-1.27	70	C	Quartz
12	7.20	6.80	4.70	0.65	0.94	0.77	-2.22	70	CB	Quartz
13	5.00	5.50	4.20	0.84	1.10	0.86	-9.45	50	CB	Quartz
14	6.50	6.40	4.10	0.63	0.98	0.74	-2.89	60	C	Quartz
15	6.00	5.80	3.50	0.58	0.97	0.71	-2.45	70	C	Quartz
16	5.00	4.20	2.30	0.46	0.84	0.63	-0.94	40	CB	Quartz
17	4.80	5.00	3.40	0.71	1.04	0.78	-4.55	80	C	Quartz
18	4.00	4.00	3.20	0.80	1.00	0.86	-4.00	90	C	Quartz
19	3.40	3.20	3.00	0.88	0.94	0.94	0.00	50	CB	Quartz
20	5.00	6.00	4.20	0.84	1.20	0.84	-14.70	40	VB	Quartz
21	2.50	2.30	1.60	0.64	0.92	0.76	-1.78	70	C	Quartz
22	8.00	8.00	4.20	0.53	1.00	0.65	-2.63	50	E	Quartz
23	5.00	4.00	3.00	0.60	0.80	0.77	0.00	60	CB	Quartz
24	4.00	4.30	3.50	0.88	1.08	0.89	-9.63	50	VB	Quartz
25	5.50	5.50	3.50	0.64	1.00	0.74	-3.18	50	E	Quartz
26	4.50	4.00	3.20	0.71	0.89	0.83	-0.82	50	VP	Quartz
27	5.00	4.70	3.00	0.60	0.94	0.73	-2.10	80	C	Quartz
28	4.00	3.80	2.00	0.50	0.95	0.64	-2.00	50	VP	Quartz

Table 1b: Pebble morphometric data of clast-supported, massive conglomerate (Gcm) sub-facies at Patigi (PAT 1E)

S/N	L	I	S	F.R (S/L)	E.R (I/L)	M.P.S.I	O-P	Roundness	Form	R.F
1	9.50	9.00	5.00	0.53	0.95	0.66	-2.05	70	C	Quartz
2	9.00	7.50	6.00	0.67	0.83	0.81	0.00	50	CB	Quartz
3	7.00	6.00	4.50	0.64	0.86	0.78	-0.64	70	C	Quartz
4	8.00	7.50	4.50	0.56	0.94	0.70	-2.01	70	C	Quartz
5	6.50	6.20	4.00	0.62	0.95	0.73	-2.34	70	C	Quartz
6	5.00	4.70	3.50	0.70	0.94	0.80	-2.10	70	C	Quartz
7	8.50	8.60	4.00	0.47	1.01	0.60	-2.46	50	VB	Quartz
8	5.00	4.80	3.50	0.70	0.96	0.80	-2.57	70	C	Quartz
9	7.00	6.00	4.00	0.57	0.86	0.72	-0.95	50	CB	Quartz
10	7.50	6.00	4.00	0.53	0.80	0.71	-0.38	50	CB	Quartz
11	6.50	5.00	3.20	0.49	0.77	0.68	-0.22	50	CB	Quartz
12	5.00	5.00	4.00	0.80	1.00	0.86	-4.00	50	C	Quartz
13	6.00	5.50	4.00	0.67	0.92	0.79	-1.67	70	C	Quartz
14	7.00	6.00	5.00	0.71	0.86	0.84	0.00	50	VP	Quartz
15	5.50	5.00	3.00	0.55	0.91	0.69	-1.64	50	CB	Quartz
16	5.50	5.20	4.50	0.82	0.95	0.89	-1.64	70	C	Quartz
17	5.00	5.00	3.00	0.60	1.00	0.71	-3.00	50	VP	Quartz
18	6.00	5.50	3.00	0.50	0.92	0.65	-1.67	50	CB	Quartz
19	6.00	5.30	4.50	0.75	0.88	0.86	-0.25	70	C	Quartz
20	7.00	6.50	4.00	0.57	0.93	0.71	-1.90	50	CB	Quartz
21	5.50	5.00	3.30	0.60	0.91	0.73	-1.64	50	VP	Quartz
22	5.50	5.00	3.00	0.55	0.91	0.69	-1.64	40	VB	Quartz

Table 1c: Pebble morphometric data of crudely bedded conglomerate (Gh) sub-facies at Baganko (BAK 1B)

S/N	L	I	S	F.R (S/L)	E.R (I/L)	M.P.S.I	O-P	Roundness	Form	R.F
1	2.30	2.00	1.40	0.61	0.87	0.75	-1.01	50	E	Quartz
2	4.00	3.50	2.90	0.73	0.88	0.84	-0.33	30	CB	Quartz
3	3.50	3.50	3.00	0.86	1.00	0.90	-4.29	40	C	Quartz
4	2.00	2.00	1.40	0.70	1.00	0.79	-3.50	40	VB	Quartz
5	2.00	2.00	1.30	0.65	1.00	0.75	-3.25	40	VB	Quartz
6	4.00	3.50	3.00	0.75	0.88	0.86	0.00	40	C	Quartz
7	2.70	2.60	2.00	0.74	0.96	0.83	-2.65	30	CB	Quartzite
8	1.70	1.50	1.20	0.71	0.88	0.83	-0.71	30	C	Quartz
9	4.10	4.20	2.30	0.56	1.02	0.67	-3.12	40	VB	Quartz
10	4.00	4.00	2.50	0.63	1.00	0.73	-3.13	30	VB	Quartz
11	4.00	4.50	3.00	0.75	1.13	0.79	-7.50	40	CB	Quartz
12	5.00	5.00	2.00	0.40	1.00	0.54	-2.00	40	E	Quartz
13	3.00	3.00	2.30	0.77	1.00	0.84	-3.83	30	VB	Quartz
14	4.00	4.50	2.20	0.55	1.13	0.65	-4.28	50	C	Quartz
15	3.00	3.00	2.40	0.80	1.00	0.86	-4.00	30	CB	Quartz
16	1.50	1.40	0.50	0.33	0.93	0.49	-1.33	40	CB	Quartz
17	1.40	1.30	0.70	0.50	0.93	0.65	-1.79	30	CB	Quartz
18	1.20	1.10	0.70	0.58	0.92	0.72	-1.75	20	C	Quartz

Table 1d: Pebble morphometric data of clast-supported, massive conglomerate (Gcm) sub-facies at Baganko (BAK 1C)

S/N	L	I	S	F.R (S/L)	E.R (I/L)	M.P.S.I	O-P	Roundness	Form	R.F
1	5.00	6.00	3.50	0.70	1.20	0.74	-8.17	70	C	Quartz
2	14.00	15.00	8.40	0.60	1.07	0.70	-4.07	80	VB	Quartz
3	10.00	8.50	5.00	0.50	0.85	0.67	-1.00	80	CB	Quartz
4	10.00	9.00	6.00	0.60	0.90	0.74	-1.50	80	VP	Quartz
5	7.00	6.80	4.00	0.57	0.97	0.70	-2.48	70	C	Quartzite
6	7.00	6.70	5.00	0.71	0.96	0.81	-2.50	60	CB	Quartz
7	5.50	5.20	4.00	0.73	0.95	0.82	-2.18	60	CB	Quartz
8	6.00	6.00	4.00	0.67	1.00	0.76	-3.33	70	C	Quartz
9	6.00	4.70	5.00	0.83	0.78	0.96	6.67	70	CB	Quartz
10	6.00	5.20	4.00	0.67	0.87	0.80	-0.67	40	VB	Quartz
11	7.00	6.00	4.00	0.57	0.86	0.72	-0.95	70	C	Quartz
12	9.00	7.00	6.00	0.67	0.78	0.83	1.11	80	VP	Quartz
13	8.00	7.00	5.80	0.73	0.88	0.84	-0.33	60	VP	Quartz
14	6.00	6.00	5.20	0.87	1.00	0.91	-4.33	50	VP	Quartz
15	5.00	5.00	2.50	0.50	1.00	0.63	-2.50	60	CB	Quartz
16	5.00	4.50	3.50	0.70	0.90	0.82	-1.17	80	C	Quartz
17	5.00	4.80	3.50	0.70	0.96	0.80	-2.57	40	CB	Quartz
18	5.00	5.50	3.40	0.68	1.10	0.75	-5.53	40	CB	Quartz
19	5.00	4.10	4.00	0.80	0.82	0.92	3.20	50	VP	Quartz
20	6.00	5.00	3.20	0.53	0.83	0.70	-0.76	40	CB	Quartz
21	5.00	5.00	3.20	0.64	1.00	0.74	-3.20	40	CB	Quartz
22	3.00	2.80	2.00	0.67	0.93	0.78	-2.00	20	CB	Quartz
23	4.20	4.30	3.20	0.76	1.02	0.83	-4.57	30	CB	Quartz

Table 1e: Pebble morphometric data of crudely bedded conglomerate (Gh) sub-facies at Baganko (BAK 1G)

S/N	L	I	S	F.R (S/L)	E.R (I/L)	M.P.S.I	O-P	Roundness	Form	R.F
1	4.50	4.60	2.50	0.56	1.02	0.67	-3.06	60	CB	Quartz
2	4.70	5.00	2.50	0.53	1.06	0.64	-3.38	40	CB	Quartz
3	4.50	4.50	3.50	0.78	1.00	0.85	-3.89	50	VP	Quartz
4	2.00	2.00	1.50	0.75	1.00	0.83	-3.75	20	C	Quartz
5	3.50	3.50	1.70	0.49	1.00	0.62	-2.43	50	E	Quartz
6	5.00	4.80	3.00	0.60	0.96	0.72	-2.40	60	CB	Quartz
7	3.50	3.20	2.40	0.69	0.91	0.80	-1.56	60	CB	Quartz
8	4.00	4.00	2.50	0.63	1.00	0.73	-3.13	40	VB	Quartz
9	6.00	5.00	3.50	0.58	0.83	0.74	-0.58	40	VB	Quartz
10	7.00	6.00	3.50	0.50	0.86	0.66	-1.07	70	CB	Quartz
11	3.50	4.00	2.00	0.57	1.14	0.66	-4.76	50	CB	Quartz
12	2.90	2.70	1.80	0.62	0.93	0.75	-1.97	50	CB	Quartz
13	4.50	3.80	3.00	0.67	0.84	0.81	-0.22	50	CB	Quartz
14	2.00	2.00	1.50	0.75	1.00	0.83	-3.75	50	VP	Quartz
15	3.50	3.00	2.70	0.77	0.86	0.89	0.96	40	C	Quartzite
16	2.70	2.30	2.00	0.74	0.85	0.86	0.53	20	CB	Quartz

Table 1f: Pebble morphometric data of matrix-supported, massive conglomerate (Gmm) sub-facies in Baganko (PAT 1E)

S/N	L	I	S	F.R (S/L)	E.R (I/L)	M.P.S.I	O-P	Roundness	Form	R.F
1	8.00	7.00	5.50	0.69	0.88	0.81	-0.69	70	C	Quartz
2	6.50	5.00	4.30	0.66	0.77	0.83	1.20	80	CB	Quartz
3	5.50	5.00	3.50	0.64	0.91	0.76	-1.59	60	C	Quartz
4	6.50	6.00	4.90	0.75	0.92	0.85	-1.41	70	CB	Quartz
5	8.70	8.00	3.50	0.40	0.92	0.56	-1.47	60	E	Quartz
6	5.50	5.00	3.90	0.71	0.91	0.82	-1.33	70	CB	Quartz
7	5.00	4.50	3.80	0.76	0.90	0.86	-0.63	70	C	Quartz
8	5.00	4.50	3.40	0.68	0.90	0.80	-1.28	50	C	Quartz
9	4.00	3.50	2.40	0.60	0.88	0.74	-1.13	50	E	Quartz
10	4.50	4.00	3.50	0.78	0.89	0.88	0.00	30	CB	Quartz
11	4.50	4.00	3.50	0.78	0.89	0.88	0.00	30	B	Quartz
12	5.00	4.50	2.50	0.50	0.90	0.65	-1.50	20	CB	Quartz
13	3.00	2.50	2.00	0.67	0.83	0.81	0.00	30	CB	Quartz
14	2.50	3.50	2.00	0.80	1.40	0.77	-20.00	30	CB	Quartz
15	4.00	4.30	2.00	0.50	1.08	0.61	-3.25	30	VP	Quartz
16	1.50	1.20	0.70	0.47	0.80	0.65	-0.58	20	VP	Quartz
17	1.50	1.60	1.00	0.67	1.07	0.75	-4.67	50	CB	Quartz
18	1.70	1.50	1.50	0.88	0.88	0.96	4.41	30	VP	Quartz
19	1.00	1.00	0.70	0.70	1.00	0.79	-3.50	20	CB	Quartz
20	1.70	1.50	1.00	0.59	0.88	0.73	-1.26	60	VB	Quartz
21	1.50	1.60	0.90	0.60	1.07	0.70	-4.00	30	VP	Quartz

Table 2: Pebble morphometric data ranges for the study samples

S/N	Location/ Sub-facies	No of Samples	F.R (S/L)	E.R (I/L)	M.P.S.I	O-P	Roundness
1	PAT-1D (Gmm)	28	0.46-0.88	0.52-1.21	0.63-1.01	-14.70-9.40	40-90
2	PAT-1E (Gcm)	22	0.47-0.82	0.77-1.01	0.60-0.89	-4.00-0.00	40-70
3	BAK-1B (Gh)	17	0.49-0.78	0.83-1.14	0.62-0.89	-4.76-0.96	20-70
4	BAK-1D (Se)	18	0.33-0.86	0.87-1.13	0.49-0.90	-7.50-0.00	20-50
5	BAK-1E (Gmm)	21	0.40-0.88	0.77-1.40	0.56-0.96	-20.00-4.41	20-80
6	BAK-1H (Gcm)	23	0.50-0.87	0.78-1.20	0.63-0.96	-8.17-6.67	20-80

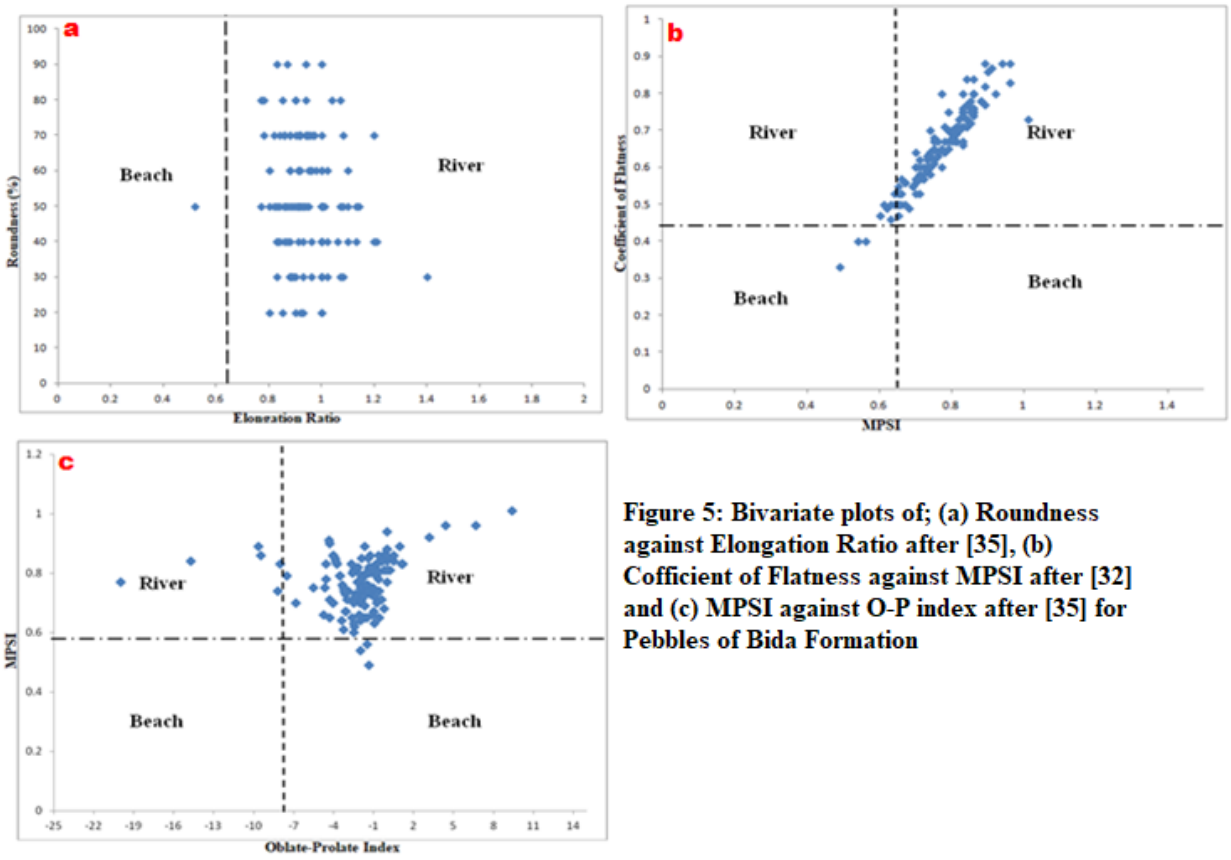

Figure 5: Bivariate plots of; (a) Roundness against Elongation Ratio after [35], (b) Cofficient of Flatness against MPSI after [32] and (c) MPSI against O-P index after [35] for Pebbles of Bida Formation

4.2 Grain Size Distribution Analysis

A total of ten representative sandstone samples (about 200g each) of matrix-supported, massive conglomerate (Gmm), crudely bedded conglomerate (Gh) and crudely bedded, massive sandstone (Se) sub-facies were collected from both locations, stored in polyethylene bags and labeled accordingly for grain size distribution analysis to obtain various textural parameters according to [36], [37] and [38]. Prior to the analysis in the laboratory, 100.0g of each sample were air-dried, gently disaggregated and homogenized using coning and quartering procedure. Each sandstone sample were then placed in the arranged set of sieve stacked vertically with the coarsest sieved at the top and finest at the bottom, with a pan using an electrical shaker for fifteen (15) minutes. At the end, each sieved sizes from different mesh size was carefully poured onto a glazed paper and weighed on electronic balance and the weight recorded. Cumulative frequency curves were plotted and phi (ϕ) values were derived from each which helped further in textural parameters; graphic mean (M_Z), inclusive graphic standard deviation (σI), inclusive graphic skewness (Ski), graphic kurtosis (KG) after [37] evaluation and interpretation which are presented in tables 3 and 4. The textural parameter values were also employed in plotting bivariate scatter diagrams for paleoenvironmental reconstruction and depositional settings determinations of sediments and sedimentary rocks within the study area.

The result of the granulometric analysis of sandstones from clast-supported, crudely bedded conglomerate (Gh) and crudely

stratified to massive sandstone (Se) sub-facies shows sediments from both locations has similar textural parameters. The textural characteristics of sandstones from Patigi fall within the very coarse to coarse sand category (-0.135 to 0.472), poorly sorted (1.329 to 1.466), graphic skewness (Sk) ranges from 0.013 to +0.171 implying symmetrical to fine skewed and graphic kurtosis (KG) value ranges of 0.672 to 0.885 suggests platykurtic. Also, the analyzed sandstone samples from Baganko have the following textural values; graphic mean (M_Z) ranging from -0.51 to 0.698 inferring very coarse to coarse grain sandstone, standard deviation (σI**)**, ranges from 0.849-1.605 with dominant values of poorly sorted grained over moderately, inclusive Graphic Skewness (Ski), range from –0.134 to +2.052 which infer varying values from coarse skewed to very fine skewed and kurtosis values ranges from very platykurtic to mesokurtic (0.585-1.018) which suggests bimodal in distribution. It is interested to know that all the analyzed sandstone are dominated of gravel and thus texturally classified as gravelly sand to sandy gravel. The dominant of poorly sorted and coarse skewed values infer that the sands are of fluvial origin.

The bivariate plots of mean grain size against standard deviation (sorting) and skewness against standard deviation collectively shows that the all the analyzed sandstone samples are fluviatile in origin which is in conformity with [17].

Table 3a: Statistical value and Interpretations of the analyzed samples of Bida Formation

Sample Name	Mean	Sorting	Skewness	Kurtosis
PAT1D	0.472 (Coarse Sand)	1.466 (Poorly Sorted)	0.013 (Symmetrical)	0.885 (Platykurtic)
PAT1E	-0.135 (Very Coarse Sand)	1.329 (Poorly Sorted)	0.171 (Fine Skewed)	0.672 (Platykurtic)
BAK1A	0.099 (Coarse Sand)	1.527 (Poorly Sorted)	0.062 (Symmetrical)	0.842 (Platykurtic)
BAK1C	0.698 (Coarse Sand)	1.289 (Poorly Sorted)	-0.134 (Coarse Skewed)	0.992 (Mesokurtic)
BAK 1F	0.274 (Coarse Sand)	1.605 (Poorly Sorted)	0.078 (Symmetrical)	1.018 (Mesokurtic)
BAK1G	-0.51 (Very Coarse Sand)	0.849 (Moderately Sorted)	2.052 (Very Fine Skewed)	0.783 (Platykurtic)
BAK1H	-0.471 (Very Coarse Sand)	1.172 (Poorly Sorted)	0.908 (Very Fine Skewed)	0.585 (Very Platykurtic)

Table 3b: Textural group and Sediment name of the analyzed samples of Bida Formation

Sample Name	Textural Group	Sediment Name
PAT1D	Gravelly Sand	Very Fine Gravelly Medium Sand
PAT1E	Gravelly Sand	Fine Gravelly Coarse Sand
BAK1A	Gravelly Sand	Very Fine Gravelly Medium Sand
BAK1C	Gravelly Sand	Very Fine Gravelly Medium Sand
BAK 1F	Gravelly Sand	Fine Gravelly Coarse Sand
BAK1G	Sandy Gravel	Sandy Fine Gravel
BAK1H	Sandy Gravel	Sandy Very Fine Gravel

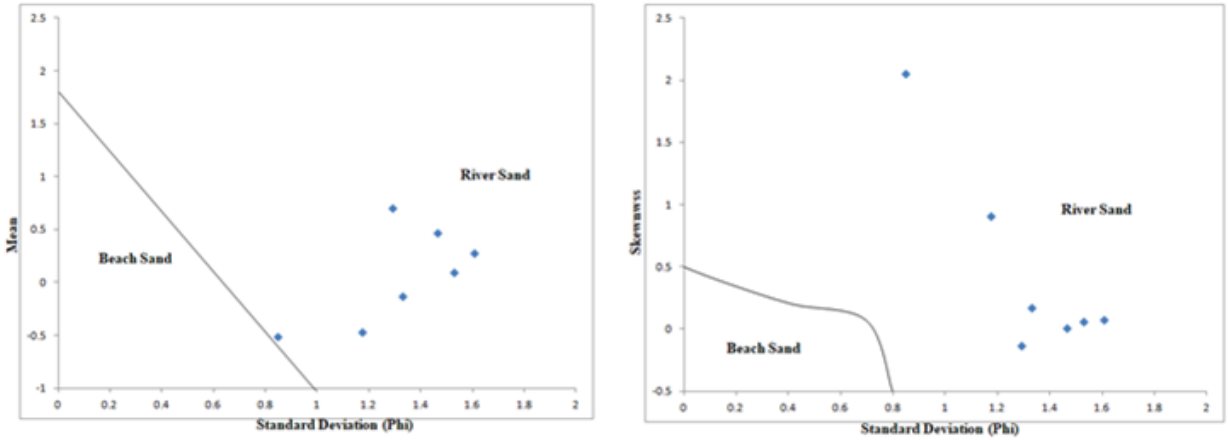

Figure 6: Bivariate plots of; (a) Mean against Standard Deviation after [39] and (b) Skewness Against Standard Devision after [40].

4.3 Palaeocurrents Data (Pebble imbrications dip direction)

Palaeocurrent study was carried out in a systematic manner involving collection of bearing of the imbricated pebbles and its orientation (dip directions) for further data interpretation. This data will help in combination with facies analysis to determine the sediment dispersal pattern, paleoflow, provenance and palaeogeography reconstruction of the basin.

A total of 20 measurements of clast imbrications were obtained from Patigi and the result shows a range from 18° to 40°W for the orientation with bearings are between 205 and 220°. The frequency distribution of set is grouped in 30° classes. A Windows based Rose program is used for the plotting of the paleocurrent data presented in table 4 to infer the paleocurrent directions during deposition of the sediments.

Table 4: Dip direction measurement of imbricated clast as a Paleocurrent data

S/N	Bearing	Dip	S/N	Bearing	Dip
1	110°	30°W	11	100°	40°W
2	110°	20°W	12	105°	30°W
3	130°	18°W	13	100°	37°W
4	120°	20°W	14	120°	38°W
5	100°	40°W	15	100°	40°W
6	120°	30°W	16	105°	35W
7	105°	38°W	17	110°	34°W
8	100°	35°W	18	120°	20°W
9	100°	36°W	19	100°	44°W
10	110°	38°W	20	110°	32°W

Range	Bearing		Dip	
	Frequency	%	Frequency	%
0 – 30	0	0.0	7	35.0
31 -60	0	0.0	13	65.0
61 -90	0	0.0	0	0.0
91 -120	15	75.0	0	0.0
121 -150	5	25	0	0.0
151 – 180	0	0.0	0	0.0
181 - 210	0	0.0	0	0.0
211 -240	0	0.0	0	0.0
241 – 270	0	0.0	0	0.0
271 – 300	0	0.0	0	0.0
301 – 330	0	0.0	0	0.0
331 – 360	0	0.0	0	0.0
	n =20	100	n =20	100

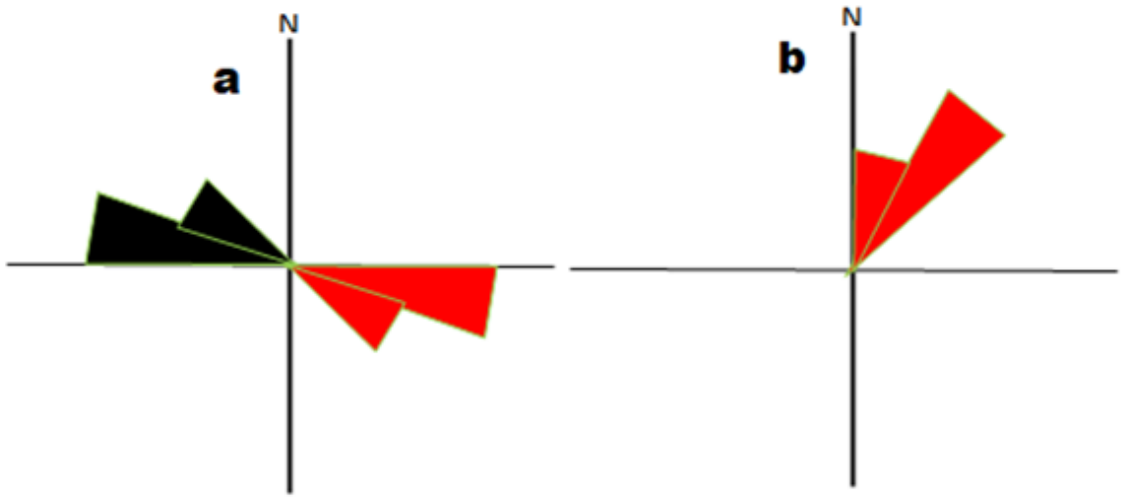

Figure 7: Rose diagram showing; (a) bearing and (b) dip direction of the tangential, tilted and imbricated pebble on the outcrop section in Patigi.

4.4 Heavy Mineral Analysis

The heavy minerals analysis was carried out on the sand fractions of sieve sizes collected on pan (0.064 mm to 0.125 mm). Heavy mineral analysis is one of the most sensitive and widely used techniques in the determination of sandstone provenance [41] because the composition of its fraction and its assemblages is chiefly controlled by the mineralogical composition of the source region [42, 43, 44]. This approach was considered to infer probable provenance as these are good indicators according to [45].

Result of heavy mineral contents (opaque and non-opaque) in the studied locations expressed in percentage (%) and the re-calculated (in %) of non-opaques is presented in table 5. The opaques occur mostly as reddish-brownish coloration and were suggested to be iron-oxide varieties (e.g. goethite, hematite and limonite) while non-opaque varieties is characterized by more zircon, tourmaline and rutile population but few garnet, biotite, sillimanite, and staurolite which are signatures that provide exceptionally useful clue to the nature of source rocks.

In the study, the heavy mineral suite comprises zircon, tourmaline, rutile, staurolite and garnet that are predominantly angular to subangular, indicating derivation from primary source of igneous granitic and metamorphic origin. Also, the varieties of the observed zircon; euhedral to subhedral, prismatic with dark boundaries, xenocrystic cores, corroded, zoning (concentric type) and those with inclusions (sillimanite) while few are fractured. Tourmaline grain varieties are mostly irregular, darkish to deep blue, golden to yellowish (dominant) while rutile mineral grain occurs as irregular, knee-shaped having brownish to deep red and orange coloration. Staurolite also presents having straw yellow colour and occurs as angular to sub-angular grains, with sub-conchoidal fractures. Garnet is characterized by its sub-rounded shape, conchoidal and etches features (Figures 8).

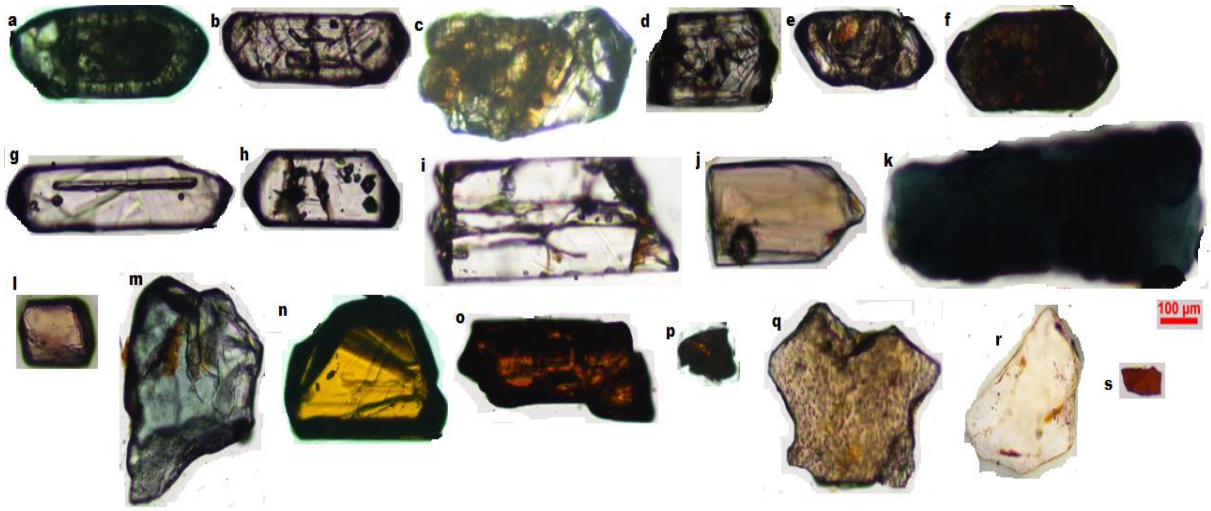

Figure 8a: Different heavy minerals types observed (under crossed nicol) in the exposed Bida Formation at Patigi; (a-i) Zircon (xenocrystic core, zoning, corroded, sillimanite inclusion and dark boundary), (j-l) Tourmaline (light brownish to bluish), (m-o) Rutile (bluish, golden, deep red colured, conchoidal and knee-shaped), (p and s) Biotite (brownish), (q) garnet and (r) Staurolite.

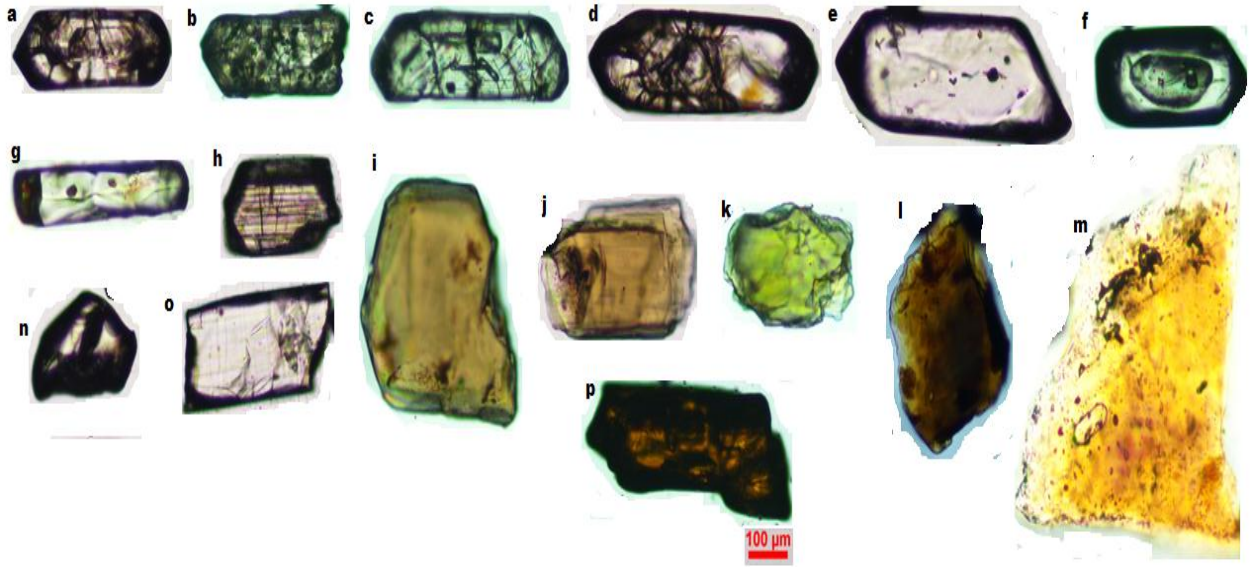

Figure 8b: Different heavy minerals types observed (under crossed nicol) in the exposed Bida Formation at Baganko; (a-h) Zircon (zoning, weathered and corroded, xenocrystic core, inclusion and dark boundary), (j-l) Tourmaline (greenish, light brownish and yellowish), (m) Staurolite (yellowish), (n-p) Rutile (dark brownish and deep brownish knee-shaped).

Table 5: Statistics for opaque and non opaque heavy minerals

Location/ Sub-facies	Mineral (%)		Recalculated (%) of Non-Opaque minerals							
	Opaque	Non-opaque	Zircon	Tour-maline	Rutile	Staurolite	Biotite	Muscovite	Sillimanite	Garnet
PAT-1D (Gmm)	60.00	40.00	29.12	9.70	43.69	12.14	0.49	0.97	1.46	2.43
PAT-1E (Gcm)	50.00	50.00	32.25	9.67	48.39	0.00	0.00	3.23	3.23	3.23
BAK-1B (Gh)	55.00	45.00	22.73	27.27	36.36	4.54	1.81	2.73	0.92	3.64
BAK-1D (Se)	60.00	40.00	5.66	30.19	37.74	13.21	3.77	5.66	0.00	3.77
BAK-1E (Gmm)	55.00	45.00	57.15	14.28	17.86	0.00	3.57	0.00	3.57	3.57
BAK-1H (Gcm)	48.00	52.00	20.41	27.21	34.01	10.20	0.68	3.41	1.36	2.72

5.0 Discussions

5.1 Paleoenvironments and Depositional Environment

The field observations and laboratory data are synthesized together in an attempt to bring out and discuss various factors and parameters that controlled the sedimentation history and environment of deposition of the sedimentary rocks in northern Bida sub-Basin. The facies within the study area is interpreted as high energy braided system with low sinuosity which represents a proximal depositional style that is probably tectonically controlled.

Generally, the observed reddish-brown colouration of the beds in both locations typically indicates deposition in continental sedimentary environments. The sediments within the study area are composed of conglomerate sandstone lithofacies which are sub-divided to clast-supported, massive conglomerate (Gcm) matrix-supported, massive conglomerate (Gmm), clast-supported, crudely bedded conglomerate (Gh) and crudely stratified to massive sandstone (Se). The interrelationship between textural distribution and depositional environments and/or processes has been used successfully to identify the depositional environments and recognize operative processes of sedimentation of ancient terrigenous deposits [40]. The assorted pebble assemblages' reveals sphericity (M.P.S.I) values higher than the sphericity line (>0.66), the oblate–prolate index range between -14.70 and 9.40, F.R. and E.R. with ranges from 0.33 to 0.86 and 0.33 to 0.88 respectively and their bivariate plots of maximum projection sphericity against oblate–prolate index, coefficient of flatness against sphericity and roundness against maximum projection sphericity after [32, 35, 46], indicates that the pebbles were deposited in a fluvial environment (Figures 6a-c). Also, according to [35, 47], dominant of compact (C) and compact bladed (CB) are most indicative of fluvial action, therefore, considering the mean geometric forms results; 40.3% compact bladed, 29.5% compact, 12.4% very platy, 11.6% very bladed, 5.4% elongate and 0.8% bladed (see Table 1), it's clearly indicated that the studied pebbles were deposited in a fluvial environment.

The grain size analysis result have similar statistical parameters for the interbedded sandstones in the both locations (see Tables 3 and 4); the coarse to very coarse grained, poorly to moderately sorted, coarse to fine skewed and very leptokurtic to mesokurtic and bivariate plots indicate that all the analyzed sandstone samples plotted within river sands (Figures 7a and 7b) which were transported mainly by rivers and deposited in a fluvial environment.

5.2 Transport history and Provenance

The analysis of imbricated pebbles at Patigi and interpretation of paleocurrent data reveals indicate mostly unidirectional paleocurrent pattern and paleo-flow direction in the northwestern and western directions indicating the source areas were on the southeastern and eastern directions respectively (Figure 5a). Also, the tangential and dip orientation of the pebbles (18-44°W) reveals deposition by river system draining mostly from southeastern and eastern part of the northern Bida sub-Basin implying relatively low channel sinuosity of the sediment contribution of Bida Formation from the source area.

It is common knowledge that grain size depends largely on current strength (velocity) of the local environment and the size of particles at source; the degree of sorting of grains is a function of the persistence and stability of energy condition. In this study, therefore, the poor sorting of the grains indicates short transport and suggests sediments derivation from first cycle of erosion and deposition.

According to [48], detrital zircons normally originate from acidic and intermediate igneous rocks whereas garnet and tourmaline are well known metamorphic rock accessory minerals and present in few less amount. The angular, euhedral zircon and greenish to bluish tourmaline characterize acid to intermediate granitic source rocks according to [49]. The knee-shaped rutile might have been derived from acid metamorphic rocks. These varying types of zircon, tourmaline is concluded to have derived from a mixed composition of provenance comprising granitic igneous rocks and low metamorphic grade rocks through “first cycle”, non-sedimentary source.

6.0 Conclusion

This study focused on the palaeogeographical, palaeoenvironmental reconstruction and provenance determination of the Bida Formation sediments exposed at Patigi and Baganko in northern Bida sub-Basin using facies, pebble morphology, grain size and heavy mineral analyses.

The investigated outcrops composed of conglomerate and sandstone lithofacies with distinctive clast-supported, massive conglomerate (Gcm) matrix-supported, massive conglomerate (Gmm), clast-supported, crudely bedded conglomerate (Gh) and crudely stratified to massive sandstone (Se) sub-facies which occur in a predictable order of coarsening-upward cycles in a fluvial environments. These litho and sub-facies characterizes an intraformational conglomerate facies association which form a distinguished channel body of gravel bar bedforms (GB) with lateral lobate type geometry. This high energy, low sinuosity, braided river deposits which are most frequent in the eastern and south-eastern part of the northern Bida sub-Basin is typical Bida Formation sediments and was due to low variation in the trend.

The combinations of result of grain size parameters, pebble morphometric and their different bivariate scatter plots have shown that Bida Formation sediments were predominance of first cycle with sediments transported and deposited in a high energy fluvial (river) setting.

The paleocurrent data from the pebble imbrications indicate a unimodal pattern which suggested a major flow towards northwestern with minor western direction. The heavy mineral suites which composed predominantly of zircon, tourmaline and rutile population with few garnet, biotite and

staurolite indicates derivation from igneous granitic and metamorphic origin.

References

[1] Ojo, S.B. (1984). Middle Niger Basin Revisited, Magnetic constraints on gravity interpretations. Nig. Min. & Geosc. Soc. Conf., Nsukka, Nigeria, Abst. pp. 52-53.

[2] Udensi, E. E. and Osasuwa, I.B. (2004). Spectra determination of depths to magnetic rocks under the Nupe Basin, Nigeria. Nig. Assoc. of Pet. Expl. Bull., v. 17, pp. 22-37.

[3] Braide, S.P. (1992). Syntectonic fluvial sedimentation in the central Bida Basin. J. Min. & Geol., v. 28, pp. 55-64.

[4] King, L.C. (1950). Outline and distribution of Gondwanaland. Geological Magazine, v. 87, pp. 353-359.

[5] Kennedy, W.Q. (1965). The influence of basement structure on the evolution of the coastal (Mesozoic and Tertiary) basins. In: Recent Basins around Africa. Proc. of the Inst. of Pet. Geol. Soc., London, pp. 35-47.

[6] Kogbe, C.A., Ajakaiye, D.E. and Matheis, G. (1983). Confirmation of rift structure along the middle- Niger Valley, Nigeria. J. Afr. Earth Sci., v. 1, pp. 127-131.

[7] Ojo, S.B. and Ajakaiye, D.E. (1989). Preliminary interpretation of gravity measurement in the middle Niger Basin area, Nigeria. In; C.A. Kogbe (ed) Geology of Nigeria, 2nd Edition, Elizabeth Publishing Co., Lagos, pp. 347-358.

[8] Murat, C. (1972). Stratigraphy and paleogeography of the cretaceous and lower tertiary in South-eastern Nigeria. In: Dessauvagie, T.F.J., Whiteman, A.J. (Eds.), African Geology. University of Ibadan Press, pp. 251–266.

[9] Adeleye, D.R. (1974). Sedimentology of the fluvial Bida Sandstones (Cretaceous) Nigeria. Sed. Geol., v. 12, pp. 1-24.

[10] Adeleye, D.R. and Desauvagie, T.F.J. (1972). Stratigraphy of the Niger Embayment near Bida, Nigeria. In: T. F. J. Dessauvagie and A. J. Whiteman (eds), African Geology, University of Ibadan Press. pp. 181-186.

[11] Ladipo, K.O., Akande, S.O. and Mucke, A. (1994). Genesis of Ironstones from the Middle Niger Sedimentary Basin, Evidence from Ore Microscopic and Geochemical Studies. J. Min. & Geol., v. 30, pp. 161-168.

[12] Abimbola, A.F. (1997). Petrographic and paragenetic studies of the Agbaja Ironstone Formation, Nupe Basin, Nigeria. J. Afr. Earth Sci., v. 25, pp. 169-181.

[13] Vrbka, P., Ojo, O.J., and Gebhardt, H. (1999). Hydraulic characteristics of the Maastrichtian sedimentary rocks of the southeastern Bida basin, Nigeria: J. Afr. Earth Sci., vol. 29(4), pp. 659-667.

[14] Ojo, O.J. and Akande, S.O. (2003). Facies Relationships and Depositional Environments of the Upper Cretaceous Lokoja Formation in the Bida Basin, Nigeria. J. Min. & Geol., v. 39, pp. 39-48.

[15] Olaniyan, O. and Olabaniyi, S.B. (1996). Facies analysis of the Bida Sandstone Formation around Kajita, Nupe Basin, Nigeria. J. Afr. Earth Sci., v. 23, pp. 253-256.

[16] Olugbemiro, R. and Nwajide, C.S. (1997. Grain size distribution and particle morphogenesis as signatures of depositional environments of Cretaceous (non ferruginous) facies in the Bida Basin, Nigeria. J. of Min. & Geol., v. 33, pp. 89-101.

[17] Ojo O.J. (2012). Depositional Environments and Petrographic Characteristics of Bida Formation around Share-Pategi, Northern Bida Basin, Nigeria. J. of Geog. & Geol., v. 4(1), pp. 224-241.

[18] Ojo, O.J. and Akande, S.O. (2012). Sedimentary facies relationships and depositional environments of the Maastrichtian Enagi Formation, Northern Bida Basin, Nigeria. J. Geog. & Geol., v. 4, pp. 136-147.

[19] Miall, A.D. (1988). Architectural elements and bounding surfaces in fluvial deposits: Anatomy of the Kagenta Formation (Lower Jurasssic), southwest Colorado. Sed. Geol., v. 55, pp. 233-262.

[20] Miall, A.D. (1990). Principles of sedimentary basin analyses. Springer Verlag, New York, pp. 667.

[21] Cant, D.J. (1982). Fluvial facies models and their significance. In P.A. Scholle and D. R. Spearing (eds). Sandstone Depositional Environments, AAPG Mem., pp. 115-137.

[22] Cant, D.J. and Walker, R.G. (1978). Fluvial processes and facies sequences in the sandy braided South Saskatchewan River, Canada. Sed., v. 25, pp. 625-648.

[23] Collinson, J.D. (1996). Alluvial sediments. In: Reading, H.G. (ed.). Sedimentary Environments: Processes, Facies and Stratigraphy. London, Blackswell Scientific Publications. pp. 37-82.

[24] Pettijohn, F.J. (1957). Sedimentary rocks. Harper and Brothers, New York, 718p.

[25] Walker, R.G. (1978): Facies models. Geo. Sci. Canada Rep. Ser., v. 1, pp. 171–188.

[26] Smith, D.G. (1988). Tidal bundles and mod couplets in the McMurray Formation, Norlhorn Alberta, Canada. Bull. Can. Pet. Geol., v. 36, pp. 216-219.

[27] Allen, J.R.L. (1982). Studies in fluvial sedimentation bars, bar complexes and sandstone sheets (low sinuosity braided streams) in the Brownstone Formation (L. Devonian) Welsch borders. Sed. Geol., v. 33, pp. 237-283.

[28] Selley, R.C. (1985): Ancient Sedimentary Environment, third ed. Cornell University Press, Ithaca, NY, pp. 317.

[29] Blair, T.C. (1987). Tectonic and hydrologic controls on cyclic alluvial fan, fluvial, and lacustrine rift basin sedimentation, Jurassic-Lower most Cretaceous Todos Santos Formation, Chiapas, Mexico. J. Sed. Petr., v. 57, pp. 845-862.

[30] Miall, A.D. (1996). The Geology of Fluvial Deposits. Springer, Berlin, pp. 582.

[31] Wenthworth, C.K. (1922). A scale of grade and class terms for classic sediments. J. Geol., v. 30, pp. 377 – 392.

[32] Stratten, J. (1973). Notes on the application of shape parameters to

differentiate between beach and river deposits in southern Africa. Trans Geol. Soc. South Afr., vol. 76, pp. 59-64.

[33] Sames, C.W. (1966). Morphometric data of some recent pebble associations and their applications to ancient deposits. J. Sed. Petr., v. 36, pp. 126-142.

[34] Luttig, G. (1962). The shape of pebbles in the continental fluviatile and marine facies. Int. Assoc. Sci. Hydr. Pub., v. 59, pp. 235-258.

[35] Dobkins, J.E. and Folk, R.L. (1970). Shape development on Tahiti-Nui. J. of Sed. Petr., v. 40, pp. 1167-1203.

[36] Folk, R.L. and Ward, W.C. (1957). Brazo River bar: A study in the significance of grain size parameters. J. Sed. Petr., v. 27, pp. 3-26.

[37] Folk, R.L. (1984). Petrology of sedimentary rocks. Hemphil, Austin, Texas, 182p.

[38] Reineck, H.E. and Singh, I.B. (1980). Depositional Sedimentary Environments. 2nd Edition, New York, Springer-Verlag, 551p.

[39] Moiola, R.J. and Weiser, D. (1968). Texture parameters: An evaluation. J. Sed. Petr., v. 38, pp. 45-53.

[40] Friedman, G.M. (1967). Dynamic processes and statistical parameters compared for size frequency distribution of beach and river sands. J. Sed. Petr., v. 37, pp. 327-354.

[41] Morton, A.C., Hallsworth, C.R. (1994). Identifying provenance specific features of detrital heavy mineral assemblages in sandstones. Sed. Geol., v. 90, pp. 241–256.

[42] Morton, A.C. (1991). Geochemical studies of detrital heavy minerals and their application to provenance studies. In. Morton, A. C., Todd, S. P. and Haughton, P. D. W. (eds) Developments in Sedimentary Provenance Studies. Geol. Soc. London, Special Publication, v. 57, pp. 31-45.

[43] Amireh, B.S. (1997): Sedimentology and paleogeography of the Regressive–Transgressive Kurnub Group (Early Cretaceous) of Jordan. Sed. Geol., v. 112, pp. 69–88.

[44] Dewey, J.F. and Mange, M.A. (1999). Petrography of Ordovician and Silurian sediments in the western Irish Caledonides: tracers of a short-lived Ordovician continent-arc collision orogeny and the evolution of the Laurentian Appalachian–Caledonian margin. In: Mac Niocaill, C., Ryan, P.D. (Eds.), Continental Tectonics. Geol. Soc. London, Special Publications, v. 164, pp. 55–107.

[45] Morton, A.C., Davies, J.R. and Waters, R.A. (1992). Heavy minerals as a guide to turbidite provenance in the Lower Paleozoic southern Welsh basin: a pilot study. Geol. Mag., v. 129 (5), pp. 573–580.

[46] Nwajide, C.S. and Hoque, M. (1982). Pebble morphometry as an aid in environmental diagnosis: an example from the middle Benue Trough Nigeria. J. of Min. & Geol., v. 19, pp. 114-120.

[47] Sneed, E.D. and Folk, R.L. (1958). Pebbles in the lower Colorado River, Texas: a study in particles morphogenesis. J. Sed. Petr., v. 66, pp. 114-150.

[48] Milner, H.B. (1962). Sedimentary petrography, 4th revised edition. Vol II: principles and applications. Allen & Unwin, London, pp. 715.

[49] Krynine, P.D. (1946). The Tourmaline group in sediments. J. Geol., v. 54, pp. 65-87.